Extended defects in InGaAs/InGaAs strain-balanced multiple quantum wells for photovoltaic applications

2002 J. Phys.: Condens. Matter 14 13367

(http://iopscience.iop.org/0953-8984/14/48/390)

INSTITUTE OF PHYSICS PUBLISHING JOURNAL OF PHYSICS: CONDENSED MATTER

J. Phys.: Condens. Matter **14** (2002) 13367–13373 PII: S0953-8984(02)54239-9

Extended defects in InGaAs/InGaAs strain-balanced multiple quantum wells for photovoltaic applications

Lucia Nasi[1], Claudio Ferrari[1], Laura Lazzarini[1], Giancarlo Salviati[1], Stefania Tundo[2], Massimo Mazzer[3], Graham Clarke[4] and Carsten Rohr[5]

[1] CNR-IMEM Institute, Parco Area delle Scienze 37/A, I-43010 Fontanini-Parma, Italy
[2] Unità INFM, Dip. Ingegneria dell'Innovazione, Via Arnesano, 73100 Lecce, Italy
[3] CNR-IME, University Campus, via Arnesano, I-73100 Lecce, Italy
[4] IQE Ltd, Cardiff, Wales, UK
[5] QPV Group, ICSTM, London SW7 2AZ, UK

Received 3 October 2002
Published 22 November 2002
Online at stacks.iop.org/JPhysCM/14/13367

Abstract

Different strain-balanced InGaAs/InGaAs multiple quantum wells (MQWs) were grown on (001) InP changing the In composition in the wells/barriers in order to extend the absorption edge beyond 2 μm for thermophotovoltaic applications. The strain increase in the structures results in the formation of isolated highly defected regions taking their origin from lateral layer thickness modulations. Experimental results are consistent with the existence of a critical elastic energy density for the development of MQW waviness. An empirical model for predicting the maximum number of layers that can be grown without modulations as a function of the strain energy stored in the MQW period is presented.

1. Introduction

By alternating compressive and tensile mismatched layers it is possible to grow structures which are locally strained, but exert no net force on the substrate [1]. The use of zero-net-strain multi-quantum-well (MQW) structures as active components of high-efficiency III–V quantum photovoltaic (PV) cells for solar and thermophotovoltaic (TPV) applications [2] has attracted a particularly large amount of interest. The strain balance (SB) technique in a quantum PV field allows a large number of QWs to be grown pseudomorphically for high-efficiency operations and at the same time offers interesting band-gap configurations for extending the absorption to longer wavelengths.

SB epitaxy on commonly available substrates, however, is very critical when the well/barrier (W/B) strain is of the order of 1% and often results in wavy growth [3, 4] which eventually leads to the formation of extended defects in the MQW with detrimental effects on the PV device performance. Although a number of works have been carried out to study the energetic and kinetic factors driving the wavy growth in strained MQWs [5], very little is

Table 1. Summary of the MQW main structural details obtained from the XRD and TEM data. N_{tot} is the entire number of periods in the MQWs and N_w the layer number at which the thickness modulations are observed to begin.

Sample No	Well strain (%)	Barrier strain (%)	Net strain (%)	N_{tot}	N_w	Defect clusters
1	0.61	−0.48	0.04	30	27	Yes
2	0.67	−0.48	0.07	10	None	No
3	0.67	−0.48	0.07	30	None	No
4	0.89	−1.35	−0.44	10	9	No
5	0.99	−0.92	0.02	30	10	Yes
6	1.09	−1.35	−0.26	10	6	Yes
7	1.18	−1.54	−0.36	10	7	Yes
8	1.18	−1.58	−0.39	10	7	Yes
9	1.33	−1.12	−0.20	10	9	No
10	1.44	−1.18	0.09	2	None	No

known about how the flat-to-rough morphology transition depends on the strain in SB systems, when varying the W/B misfit over a wide range.

In this paper we report a structural study of novel structures based on InGaAs/InGaAs SB MQWs grown on InP substrates for TPV applications. The nature of the defects and the mechanisms of their formation are analysed and discussed in terms of the strain incorporated in the structures.

2. Experimental details

We have studied MQWs consisting of 30 repetitions of SB $In_yGa_{1-y}As/In_xGa_{1-x}As$ inserted in the intrinsic region of InGaAs-based p–i–n structures and several SB MQWS with only ten repetitions grown on (100) InP substrates by metal–organic vapour phase epitaxy (MOVPE). The compositions and thickness of the well and barrier layers were designed to extend the absorption edge between 1800 and 2000 nm while achieving the zero-net-strain condition [1].

The x-ray characterization was performed by the methods of double-crystal x-ray topography (XRT) and high-resolution x-ray diffraction (HRXRD) in the Cu Kα 004 symmetrical and the 335 asymmetrical geometries using a Philips high-resolution x-ray diffractometer. Transmission electron microscopy (TEM) was carried out in a Jeol 2000FX operated at 200 kV. Observations were made on (001) plan-view and $\{110\}$ cross-section specimens, with $\boldsymbol{g} = 220$ and 002, which are known to be sensitive to strain field and chemical composition respectively.

3. Results

The sample details in terms of the MQW strain arrangement are given in table 1. All the structures were grown under the same growth conditions except samples 9 and 10 which are deposited at a lower temperature. The experimental values of the W/B misfit strain and the MQW net strains (calculated by accounting for the different elastic properties of the layers) are reported. The matching was imperfect, the MQWs being either in compressive or in tensile strain with respect to the InP substrate. All the data were calculated by using the indium composition and thickness values of the W/B layers obtained from the HRXRD measurements. Figure 1 shows, as an example, the experimental and simulated double-crystal rocking curves obtained from sample 5. In this sample, the barycentre of the superlattice zeroth-order peak is displaced by approximately +450 arcsec from the substrate peak corresponding to a net tensile-

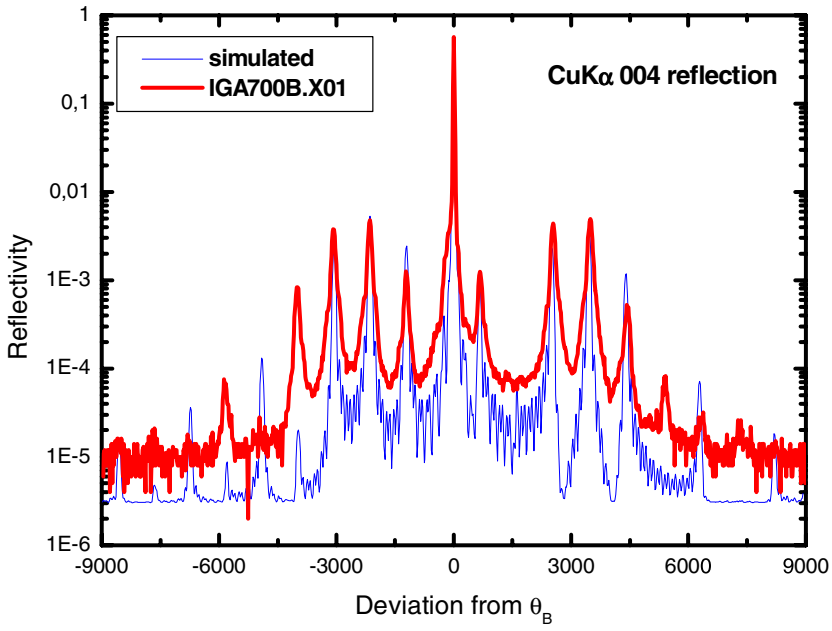

Figure 1. Experimental and simulated double-crystal x-ray rocking curves from sample 5. (This figure is in colour only in the electronic version)

strained MQW. The superlattice peak sharpness demonstrates a good interface planarity and a very stable composition and period along the structure. The agreement between experimental and simulated profiles allowed us to determine with high accuracy the composition of InGaAs wells and barriers. It is worth noting that the opposite strains of barriers and wells in the superlattice lead to diffraction profiles with two large envelopes of SL peaks on opposite sides of the substrate peak. The W/B strain increase results in a larger separation of the two envelopes and a broadening of the superlattice peaks which is consistent with the onset of the period instabilities revealed by TEM.

The presence of structural defects on a large scale has been checked by means of XRT. No misfit dislocations (MDs) were found in any sample investigated. A high density of randomly distributed defects were revealed by XRT when the strain in the W/B layers becomes higher (not shown here). $\boldsymbol{g} = 002$ TEM cross-section observations show that the epitaxial growth front in the MQWs is flat up to a certain thickness, where a change in the growth mode causes MQW waviness and may result in the formation of highly defected regions. The layer at which the thickness modulations are observed to begin, N_w, is reported in table 1.

The details on the formation and development of these defects can be summarized as follows:

(i) The MQW thickness modulations always start in the tensile barrier layers as clearly shown in the dark-field $\boldsymbol{g} = 002$ TEM images (figures 2(a), (b)).

(ii) The subsequent compressive layer tends to smooth the tensile layer 3D growth front (figure 2(a)). However, this layer is not thick enough to prevent the following barrier layer from being influenced by the strain field originating from the ripples below. As a consequence the undulations propagate vertically through the MQW structure with increasing amplitude and develop in antiphase with each other.

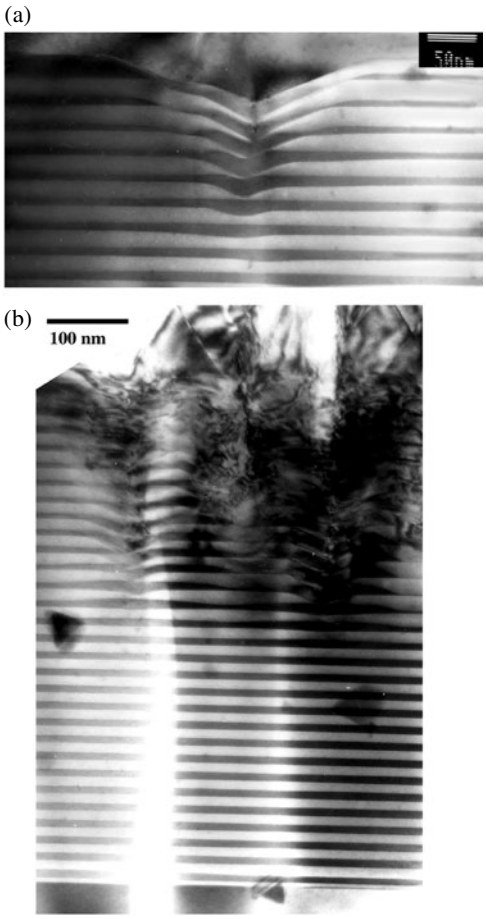

Figure 2. (a), (b) Bright-field ($\boldsymbol{g} = 002$) TEM cross-sections showing the development of wavy growth in two different structures investigated. Wells and barriers correspond to darker and brighter layers respectively.

(iii) The extended defects may arise as a consequence of local stress concentration in the MQW regions exhibiting significant local rippling (figure 2(b)). They are always arranged in clusters which do not 'talk to each other' and consist of stacking faults and dislocations threading up to the free surface. Inside these defect regions, the growth of the above layers is inhibited, causing deep depressions on the surface (revealed by AFM measurements, not shown). Away from the clusters, the MQWs present flat layers with sharp well and barrier interfaces.

The cluster arrangement of the defects is shown by TEM plan-view observations (figure 3). The black/white contrast fringes surrounding the clusters have been ascribed to strain field modulation due to the underlying MQW rippling. This conclusion is supported by the inversion of contrast occurring when the sign of the operating $\boldsymbol{g} = 220$ is reversed. In fact, the lateral thickness fluctuation in the MQW forms a columnar structure with regions of different W/B thickness ratio which results in the lateral succession of regions under compressive and tensile strain [6]. It was found, by AFM investigations, that the density of the surface depressions associated with the defect clusters increases as the strain in the wells/barriers increases, while

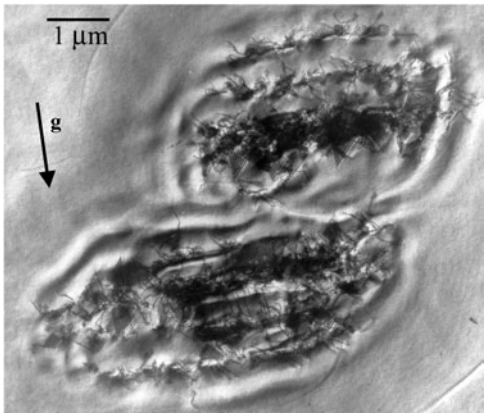

Figure 3. A dark-field ($g = 220$) TEM plan-view image of defect clusters in sample 1.

their lateral dimensions strictly depend upon the number of layers in the stack that break down as a consequence of defect formation. The defect-related depressions are always elongated along one of the two ⟨110⟩ directions.

Spectrally resolved CL measurements show that the indium content increase in the wells (from samples 1–10) shifts the emission peak wavelengths from 1520 to 2040 nm at RT. A high non-radiative recombination activity of the defect clusters is revealed by both CL and EBIC analysis. Nevertheless, they have a limited effect on the cell dark current, while they appear to be correlated with the dramatic drop of the photocurrent even at a very low forward bias voltage [10]. Work is in progress to understand the CL and EBIC contrast at the cluster boundaries in terms of the impurity gettering phenomenon.

4. Discussion

On the basis of the empirical model for the strain relaxation developed by Drigo *et al* [7] and by using the HRXRD indium composition data, the critical thicknesses for the onset of plastic relaxation mechanisms in multilayers have been calculated. For all the samples investigated, the thicknesses of either each layer or the total set of MQW turn out to be lower than the critical values for the introduction of MDs between individual layers and between the whole set of MQW and the substrate, in agreement with our experimental results. As a consequence, the presence of the defect clusters is not dependent on the net MQW strain but only on the difference between the W/B mismatches. This finding, together with the localized nature of the defects, rules out the possibility of the biaxial strain being responsible for their formation.

To understand the origin of the extended defects and their correlation with the W/B strain, we start from the fact that one layer in the MQW (for whatever reason) exhibits wavy growth. In our structures, tensile layers seem to be responsible for this effect—in agreement with other findings [3, 8]. Due to the elastic relaxation phenomena, the growth front of a wavy layer exhibits lattice parameter fluctuations, the thickest regions being partially relaxed compared to the thinnest ones. The rapid increase of the waviness amplitude observed in SB structures is ascribed to the opposite preferential growth regions of compressive and tensile layers during the growth on non-homogeneous strained surface [9]. The highly stressed columnar regions become a source of the observed extended defects when the misfit between well and barrier increases. This conclusion is confirmed by the defect arrangement in the clusters (figure 3),

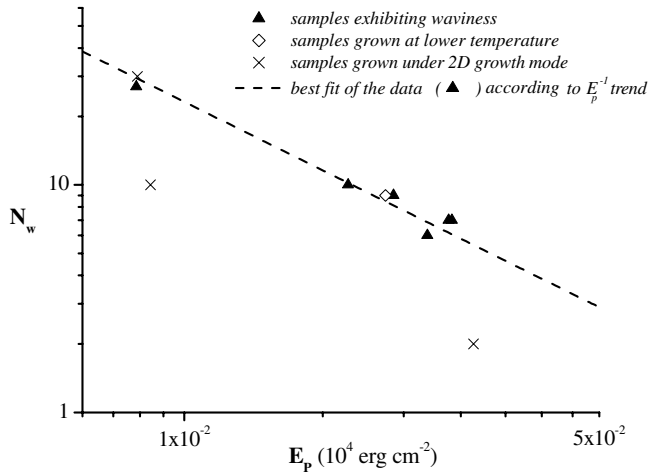

Figure 4. Experimental values of N_w found by TEM reported as a function of the strain energy density per period, E_p.

showing a clear spatial correlation between the dislocation nucleation sites and the strain boundaries due to MQW lateral modulations.

It is well known that the evolution from planar to wavy growth is a complex phenomenon which involves both kinetic and energetic arguments [5]. We expect for all the samples grown under the same growth conditions some dependence of the flat-to-rough morphology transition on the strain arrangement in the MQWs. It appears from table 1 that increasing the W/B strain results in a decrease of the total thickness at which the onset of wavy growth occurs. This suggests that the strain energy density stored in the structure plays a crucial role in the development of the growth mode. Assuming the existence of a critical elastic energy, E_c, for the roughness transition, it might be expected that the layer at which wavy growth should start can be simply predicted by the relation

$$N_w = E_c/E_p \tag{1}$$

where E_p is the elastic energy density accumulated in one period. In the plot shown in figure 4 the experimental values of N_w found by TEM are reported as a function of the strain energy density per period. E_p has been calculated taking into account the differences between the elastic properties of the layers:

$$E_p = (A_w \varepsilon_w^2 t_w + A_b \varepsilon_b^2 t_b) \tag{2}$$

where $\varepsilon_{w,b}$ and $t_{w,b}$ are the strain and the thickness of the wells and barriers calculated by using the XRD data while the $A_{w,b}$ are functions of the elastic stiffness coefficients of each layer. The E_p^{-1}-dependence of N_w is clearly reflected in the data, as revealed by the best empirical fit, according to equation (1), represented by the dashed line in figure 4.

This result thus supports the hypothesis of the existence of a critical strain energy for the flat-to-rough transition. This model accounts also for the samples investigated that do not present undulations, for which the total numbers of MQW layers have been marked with crosses (figure 4). Taking into account the experimental error range, they are positioned below the transition curve, since their strain energy density has not overcome the critical value. It is worth noting that sample 9, marked with an empty diamond in the diagram, also presents undulated interfaces at the N_w-value predicted by this model although it was grown at a lower

growth temperature. However, in this case the undulations are very small in amplitude and no extended defects were produced. In any case, this behaviour is not in agreement with the predicted temperature dependence of the roughening transition in III–V MQWs, $E_c \sim T^{-1/2}$, found by Bangert *et al* [5]. Further investigations are in progress to study the influence of the growth temperature on the wavy growth mode in this kind of structure.

5. Conclusions

The mismatch increase in SB InGaAs/InGaAs MQWs is effective in shifting the absorption wavelength to 2 μm, but results in the development of surface roughness. Lateral thickness modulation enlarges its amplitude as growth proceeds, leading to the formation of defect clusters. For samples grown under the same conditions, the predominant parameter controlling this process is found to be the elastic energy density. The maximum number of layers in a stack that do not exhibit thickness modulations N_w follows an E_p^{-1}-relationship that is consistent with the existence of a critical elastic energy per unit surface for the flat-to-rough morphology transition. These results suggest an upper limit to the wavelength value that can be achieved in TPV cells using the SB technique.

References

[1] Ekins-Daukes N J, Zhang J, Bushnell D B, Barnham K W J, Mazzer M and Roberts J S 2000 *Proc. 28th IEEE Photovoltaic Specialists Conf. (Anchorage, AK, USA)* (New York: IEEE)
[2] Rohr C, Connolly J P, Ekins-Daukes N, Abbott P, Ballard I, Barnham K W J, Mazzer M and Button C 2002 *Physica E: Low-dimensional Systems and Nanostructures* **14** 158
[3] Ponchet A, Rocher A, Ougazzaden A and Mircea A 1994 *J. Appl. Phys.* **75** 7881
[4] Mitsuhara M, Ogasawara M and Sugiura H 2000 *J. Cryst. Growth* **210** 463
[5] Bangert U, Harvey A J, Dieker C, Hartdegen H, Vesca L and Smith A 1995 *J. Appl. Phys.* **78** 811
[6] Lazzarini L, Nasi L, Ferrari C, Salviati G, Mazzer M, Passaseo A and Barnham K W 2001 *Inst. Phys. Conf. Ser. 169* 109
[7] Drigo A V, Aydinli A, Carnera A, Genova F, Rigo C, Ferrari C, Franzosi P and Salviati G 1989 *J. Appl. Phys.* **66** 1975
[8] Kröner P, Baumeister H, Rieger J, Veuhoff E, Marti O and Heinecke H 2000 *J. Cryst. Growth* **209** 424
[9] Ponchet A, Rocher A, Emery J Y, Starck C and Goldstein N 1993 *J. Appl. Phys.* **74** 3778
[10] Tundo S, Mazzer M, Lazzarini L, Nasi L, Torsello G, Diso D, Clarke G, Rohr C and Barnham K 2002 *Mater. Sci. Technol.* to be published